ARTICLE   OPEN

Disentangling the North Pacific Meridional Mode from tropical Pacific variability

Ingo Richter [1✉], Malte F. Stuecker [2,3], Naoya Takahashi [3] and Niklas Schneider[2,3]

Variations of sea-surface temperature (SST) in the subtropical North Pacific have received considerable attention due to their potential role as a precursor of El Niño-Southern Oscillation (ENSO) events in the tropical Pacific as well as their role in regional climate impacts. These subtropical SST variations, known as the North Pacific Meridional Mode (PMM), are thought to be triggered by extratropical atmospheric forcing and amplified by air-sea coupling involving surface winds, evaporation, and SST. The PMM is often defined through a statistical technique called maximum covariance analysis (MCA) that identifies patterns of maximum covariability between SST and surface winds. Here we show that SST alone is sufficient to reproduce the MCA-based PMM index with near-perfect correlation. This dominance of the SST suggests that the MCA-based definition of the PMM may not be ideally suited for capturing two-way wind-SST interaction or, alternatively, that this interaction is relatively weak. We further show that the MCA-based PMM definition conflates intrinsic subtropical and remote ENSO variability, thereby undermining its interpretation as an ENSO precursor. Our findings indicate that, while air-sea coupling may be important for variability in the subtropical North Pacific, it cannot be reliably identified by the MCA-based definition of the PMM. This highlights the need for refined tools to diagnose variability in the subtropical North Pacific.

INTRODUCTION

Climate variability in the subtropical North Pacific has been widely studied[1–7]. While the variability of Pacific sea-surface temperatures (SSTs) in the low latitudes is dominated by El Niño-Southern Oscillation[8–10] (ENSO), numerous studies have suggested that the subtropical North Pacific may be home to an independent variability pattern that is maintained by the two-way coupling (hereafter just "coupling") between surface winds, evaporation, and SST (the so-called wind-evaporation-SST or WES feedback[11,12]; see "Methods" for a short description), and forms a central part of the North Pacific Meridional Mode[1] (PMM hereafter). In its positive phase, the PMM pattern consists of warm SST anomalies that extend southwestward from the California coast toward the western equatorial Pacific, accompanied by a weakening of the northeast trade winds (Fig. 1a). The initial forcing of this pattern is from intrinsic atmospheric variability in the midlatitudes that extends into the subtropics[1].

The PMM is known to have its own regional climate impacts, such as influencing droughts in California[13] and modulating eastern Pacific hurricane occurrence[14], but has probably garnered wider attention due to its potential role as a precursor of ENSO[15–18]. It has been shown that atmospheric variability in the extratropical North Pacific, which is largely stochastic in nature[4], can seed the development of the PMM during northern hemisphere winter[19] (December-January-February or DJF). As the PMM matures in spring (March-April-May or MAM), it propagates toward the equator as a coupled wind-SST mode, an intrinsic property of the WES feedback[11,12]. When the SST pattern approaches the equator, the accompanying weakening of the trade winds can initiate the development of an El Niño event that typically matures in the following winter (DJF) and couples tropical winds, SST and ocean circulation. Predicting El Niño from MAM is notoriously difficult[16]. It has been suggested that the PMM may help to overcome this ENSO predictability barrier[2,20] and enable skillful

ENSO predictions at longer lead times. This could also offer a theoretical framework for understanding how stochastic atmospheric variability in the North Pacific can influence ENSO.

RESULTS

The problem of defining the PMM

Since the PMM is situated just northeast to the region of intense ENSO activity, a major problem has been how to diagnose PMM variability without contamination by the strong ENSO signal. The conventional approach has been to first remove the ENSO signal by linearly regressing out an indicator of ENSO activity called the cold tongue index (CTI; see "Methods"). In the second step, a statistical technique called maximum covariance analysis (MCA; also known as singular value decomposition or SVD; see "Methods") is applied to find the dominant pattern of coupled SST-wind variability. The MCA yields two spatial patterns and temporal expansion coefficients (one for each of the two input fields) that form the basis of the PMM definition[1,21]. Studies of the PMM often use the SST pattern to define an index of PMM variability[1,2,6,7,14,17,22] (see "Methods"). We will refer to this index as the PMM index, or, where clarification is necessary, as the reference PMM-T index. Two assumptions are key to the MCA-based PMM definition: (1) regressing out the CTI is an effective way of removing ENSO variability; (2) MCA can reliably identify coupled SST-wind variability in the subtropics. While assumption (1) has been examined to some extent[1,2,22,23], assumption (2) has received little attention. In the following we provide further evidence that assumption (1) is problematic, and show that there are caveats to assumption (2) as well. This has important implications for how we can diagnose coupled variability in the subtropical North Pacific, and also raises questions about the utility of the PMM as an independent precursor of ENSO.

[1]Application Laboratory, Research Institute for Value-Added-Information Generation, Japan Agency for Marine-Earth Science and Technology, Yokohama, Japan. [2]Department of Oceanography, School of Ocean and Earth Science and Technology, University of Hawai'i at Mānoa, Honolulu, HI, USA. [3]International Pacific Research Center, School of Ocean and Earth Science and Technology, University of Hawai'i at Mānoa, Honolulu, HI, USA. ✉email: richter@jamstec.go.jp
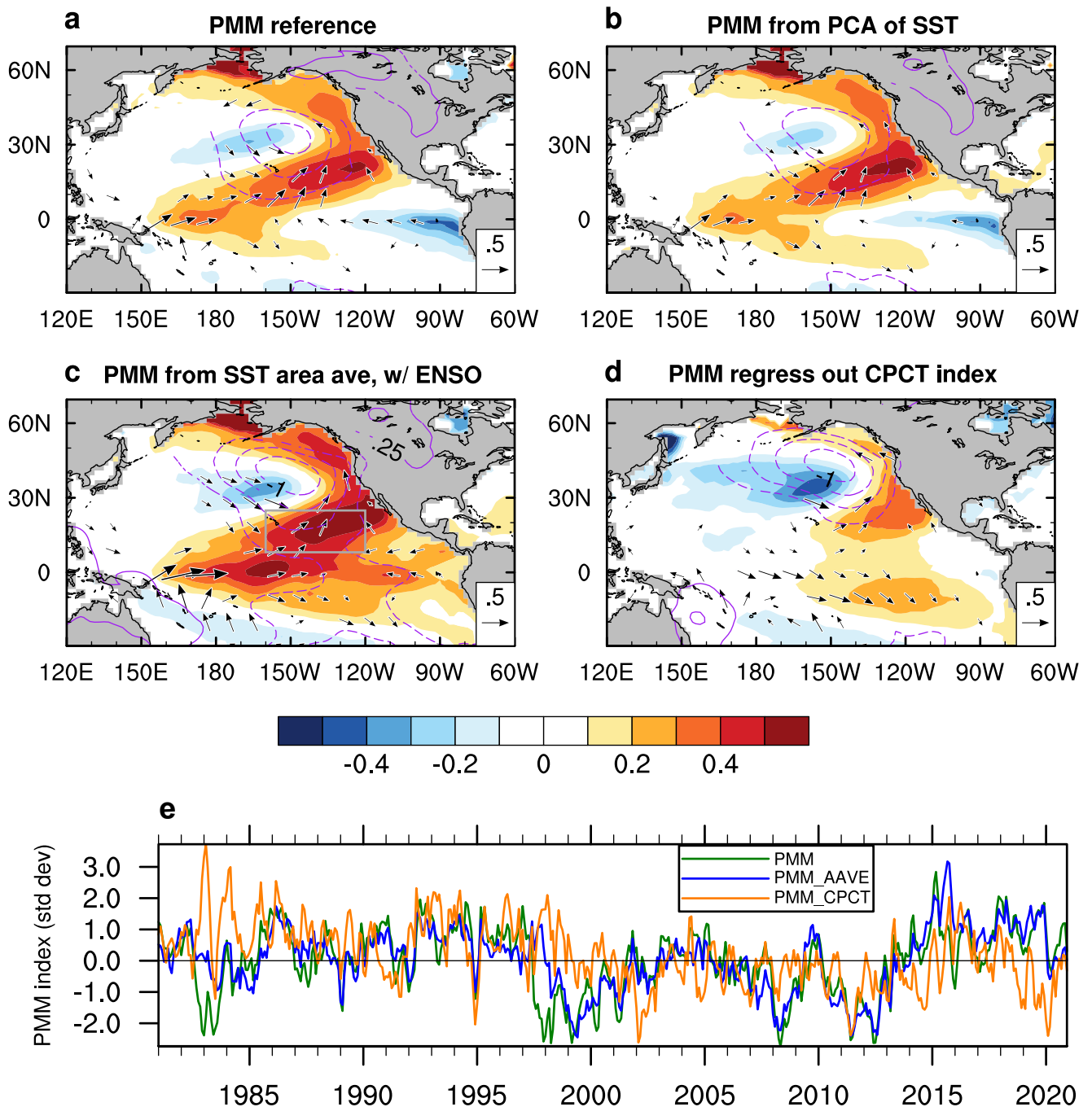
Fig. 1 The reference PMM-T and alternative indices. a Regression of the Pacific Meridional Mode (PMM) index (derived via MCA) onto anomalies of SST (°C, shading), surface winds (m s⁻¹, vectors), and sea-level pressure (contours, interval of 0.25 hPa). Negative contour lines are dashed and the 0-contour line is omitted. Only values significant at the 95% confidence level are shown. **b** Similar to (**a**), but for the expansion coefficient of a principal component analysis of SST (PMM_EOF). **c** Similar to (**a**), but for an index that is simply the area average of SST anomalies in the gray box, and without removing ENSO variability beforehand. **d** Like (**a**), but using a more thorough way of removing ENSO variability (see text). **e** Time series of three of the indices in (**a**), (**c**), and (**d**), normalized by their respective standard deviations. The time series of (**b**) is not shown as it is very similar to that of (**a**). All fields are from the NCEP/NCAR Reanalysis.

Caveats regarding the use of MCA for identifying coupled wind-SST variability in the subtropical North Pacific

The PMM is thought to rely on the WES feedback, which is distinct from the Bjerknes feedback[24] which governs equatorial Pacific variability and ENSO. By considering the coupled variability of SST and surface winds, the MCA aims to diagnose the coupled

processes that underlie the PMM and its equatorward propagation. Statistical analysis of SST alone, however, yields a pattern that is very similar (Fig. 1b; based on principal component analysis (PCA) as described in "Methods") to the one derived by MCA (Fig. 1a). The patterns of SST, wind, and sea-level pressure (SLP) are correlated with the original PMM patterns at 0.97 to 0.98, while the

SST expansion coefficient correlates with the PMM SST index (defined as the expansion coefficient of the SST pattern) at 0.95 (all pattern correlations significant above the 99.9% level, i.e., P-value < 0.001). Further sensitivity tests of the MCA reveal, that the MCA SST pattern is rather insensitive to either replacing Pacific winds with those from a remote area or to swapping the first and second half of the SST record (Supplementary Note 1 and Supplementary Fig. 4), again highlighting the dominance of the SST field. Thus, the surface winds only make a very small contribution to the reference PMM-T index. This suggests that the MCA of three fields can be replaced by PCA of only one field, SST, without much loss of information (90% variance explained). Indeed, even a simple box average of SST (PMM_aave; Fig. 1c) captures a substantial portion of the PMM variability, with the patterns correlated at ~0.95 and the time series at 0.90 (Supplementary Fig. 1b; P-value < 0.001 for both pattern and temporal correlations). Even when the ENSO influence is not regressed out prior to calculating the area average, the similarity with the reference PMM-T index and its patterns is high (Fig. 1c), with pattern correlation values of 0.80 for SST and wind fields, and 0.78 for SLP (P-value < 0.001).

Previous studies have raised concerns about the use of MCA for identifying coupled variability patterns[25,26]. In particular, it has been argued that the two patterns produced by MCA either explain little of the total covariability or, alternatively, are dominated by the EOFs of the individual fields, in which case they contain no new information[25]. Our analysis suggests that the reference PMM SST pattern falls into the latter category: it contains little information that cannot be gathered from the consideration of SST alone. Another possibility is that the MCA actually works well but that the SST-wind coupling is weak due to atmospheric noise.

The PMM wind pattern is less well represented by a PCA of wind only (Supplementary Fig. 2). Nevertheless, the PMM wind index, too, can be approximated by a simple area average of SLP in the subtropical North Pacific (Supplementary Fig. 2c). This SLP area average is correlated to the subtropical SST area average (Fig. 1c) in much the same way as the reference PMM SST and wind indices (Supplementary Fig. 3), with highest correlation when the former leads the latter. SLP is influenced by SSTs but also feeds back on them through its control of near-surface winds and latent heat flux. It is therefore not surprising that an area average of SLP can stand in for 10 m winds. This is supported by the high similarity of the wind patterns in Supplementary Fig. 2a, c. Using SLP instead of 10 m winds can be beneficial, as the latter is more easily measured. We note that the relation between SLP and surface winds is complicated by the influence of vertical mixing[27], which may also be an aspect of the WES feedback that deserves further study.

The singular value of the PMM MCA pattern passes a bootstrap test (see "Methods") with a p-value of < 0.001. Further analysis, however, suggests that this test may be too permissive and thus not sufficient to establish a statistically significant relation (see Supplementary Note 2 and Supplementary Fig. 4d).

The problem of incomplete removal of the ENSO influence

The PMM is considered to be largely independent of ENSO because it relies on a different type of air-sea interaction, namely the WES feedback. ENSO is an equatorial Pacific phenomenon but has worldwide impacts, including in the subtropical North Pacific[23]. Therefore, in the commonly used PMM definition, the ENSO signal is removed by regressing out the CTI from all fields prior to analysis[1]. The averaging area for this ENSO index extends from the date line to the eastern equatorial Pacific.

Since the original work defining the PMM was published, an additional type of El Niño has been identified that is centered in the central equatorial Pacific, variously referred to as El Niño
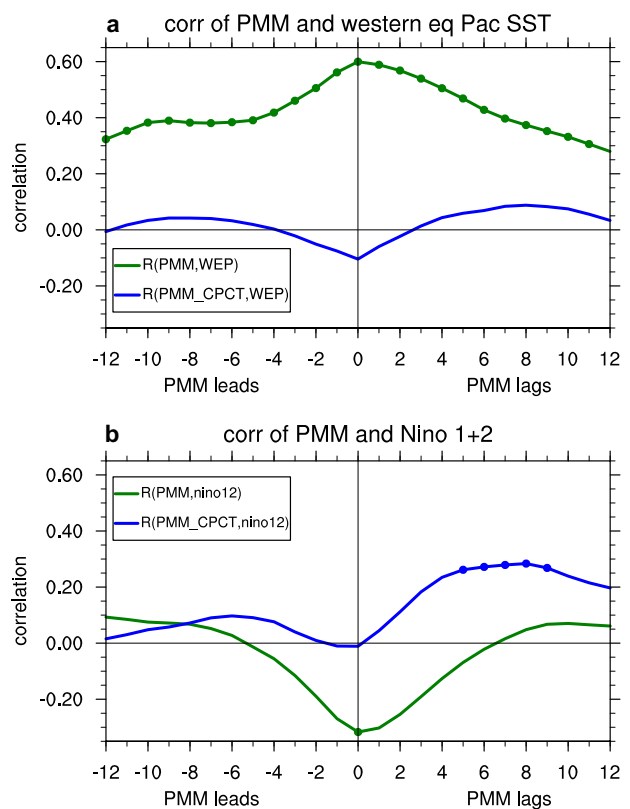

Fig. 2 Incomplete ENSO removal in the reference PMM-T index. a Lagged regressions of SST in the western equatorial Pacific (150°W-180°, 5°S-5°N) for the reference PMM-T index (green line) and the PMM_CPCT (blue line), which uses a more through method for removing ENSO prior to the PMM calculation. Negative lags indicate that the PMM leads the SST index and vice versa. Values that are statistically significant at the 95% level, based on a two-tailed Student's t-test, are marked by a filled circle. **b** Like (**a**), but for the Niño 1+2 index (SST averaged over 90°-80°W, 10°S-0°). All fields are from the NCEP/NCAR Reanalysis.

Modoki or Central Pacific (CP) Niño, and which is distinct from the canonical El Niño, which is centered in the eastern equatorial Pacific and also referred to as Cold Tongue (CT) Niño[28,29]. Considering the geographical location of the CP Niño, it is obvious that it cannot be completely removed by regressing out the CTI; indeed, it has been shown that two independent indices are needed to account for both flavors of ENSO[29]. This, however, means that the standard PMM index is contaminated by the CP ENSO signal, a fact that is apparent in the lagged correlations of the PMM and SST in the western equatorial Pacific (Fig. 2). Correlations at lag 0 are about +0.6 and remain statistically significant (P-value < 0.05) at all lags from −12 to +12 months. Moreover, correlations are roughly symmetric around the peak at lag 0. Thus, it is difficult to argue that the PMM is a precursor of CP ENSO, as has often been done in the literature. Rather, CP ENSO is built into the PMM by definition, an issue that has previously been raised[23]. We further note that contamination by the ENSO signal may also affect statistical prediction models based on linear inverse modeling (LIM; see "Methods"), which can be used to identify optimal initial SSTs (comprised of a number of non-orthogonal damped eigenmodes) for ENSO development (i.e., precursors) under stochastic forcing[30–32]. Whereas the extratropical portion of the precursor, which resembles the PMM, is often emphasized[30–32], the precursor includes an SST signal in the central equatorial Pacific. This indicates that LIM, too, may not be able to clearly separate extratropical and tropical ENSO precursors.

One could argue that CP variability is actually part of the PMM itself because previous studies, as well as the present one, have shown a close correspondence between CP ENSO and the PMM. It is certainly possible to define the PMM in this manner but, in that case, it becomes difficult to interpret the PMM as an ENSO precursor. This is because it has been shown here and elsewhere[23] that the PMM and CP ENSO have their highest correlation at lag 0. Consistently, it has been found that the PMM is not very useful in the prediction of CP ENSO[16]. More importantly, many studies indicate that the PMM is a subtropical phenomenon that relies on thermodynamic air-sea coupling (WES feedback)[1–3,22,33] while CP ENSO is an equatorial phenomenon that relies on dynamic air-sea coupling (Bjerknes feedback). We therefore believe that the PMM should be clearly separated from tropical variability.

The CTI not only fails to remove CP ENSO, it also leaves out a small area between 90°W and the South American coast. Interestingly, this area, just off Peru, is precisely where El Niño was originally discovered (first by local fishermen, then by scientists[34,35]), and has been defined as the Niño 1 + 2 region (see "Methods"). Regressing out the CTI leaves substantial ENSO-related variability in this region, and this is shown by the cold SST anomalies in the regression patterns (Fig. 1a, b) and in the lagged correlations of the PMM and Niño 1 + 2 indices (Fig. 2b).

A study by Takahashi et al.[29] recommends characterizing CP and CT variability by two indices that are roughly orthogonal to each other. We refer to this index pair as the CPCT index. When this index is regressed out instead of the CTI before performing MCA, both the cold and warm SST anomalies in the western and eastern equatorial Pacific, which characterize the reference PMM pattern (Fig. 1a), are absent (Fig. 1d), and the wind anomalies over the western equatorial Pacific (130°W-160°E, 5°S-5°N) weaken from 0.25 to 0.10 m/s. In the North Pacific (north of 20°N), on the other hand, the pattern remains quite similar to that of the reference PMM, although the positive SLP anomalies over the Gulf of Alaska are missing. Furthermore, positive SST anomalies emerge in the southeastern Pacific, leading to a pattern that is roughly symmetric about the equator. The lagged regression of the PMM and PMM_CPCT indices with SST in the western equatorial Pacific (Fig. 2a) confirms that regressing out the CPCT index pair effectively removes the CP ENSO signal from the PMM, with correlations not exceeding the 95% significance level for any lead time. The time series of the PMM_CPCT index (Fig. 1e) shows strong differences with the PMM index around the 1982/1983 and 1997/1998 extreme El Niño events, which raises the possibility that the differences in the PMM and PMM_CPCT patterns are mostly due to those extreme events. By excluding strong ENSO years from the MCA[1] we have verified that this is not the case; the patterns remain almost unchanged (not shown).

Lagged regressions of SST, winds and SLP on the MAM PMM and PMM_CPCT indices show a conspicuous difference in the evolution of these fields (Fig. 3). Both the PMM and the PMM_CPCT start with negative SLP anomalies in the North Pacific that extend into the subtropics and are accompanied by a weakening of the northeast trade winds. However, while the PMM shows SST and wind anomalies extending into the western equatorial Pacific during MAM, the PMM_CPCT does not: The SST anomalies are confined to the subtropics and the western equatorial wind anomalies are much weaker. Consistently, the PMM progresses to El Niño-like conditions toward the end of the year, whereas the PMM_CPCT does not, which indicates a weaker link between PMM-like patterns and subsequent ENSO development.

The lagged regressions of the PMM_CPCT with the Niño 1 + 2 index (Fig. 2b) reveals a further factor complicating ENSO removal, which is the autocorrelation of ENSO variability. While regressing out the CPCT index pair leads to the complete removal of the Niño 1 + 2 variability at lag 0, correlations reassert themselves at both increasing and decreasing lags, indicating the limits of regressing out the simultaneous ENSO signal; this includes the possibility of

equatorial SST anomalies in the preceding season influencing PMM development. In addition, ENSO variance is more pronounced in winter than in other seasons. Therefore, a more thorough procedure for regressing out ENSO-related variability would have to account for its seasonality.

Incomplete ENSO removal is also evident in Fig. 3b, which shows positive SST anomalies in the eastern equatorial Pacific in DJF, before the peak of the PMM. These CT El Niño-like SST anomalies may explain the more meridionally symmetric SST distribution about the equator, and the northward shift in the North Pacific SLP anomalies, both of which are consistent with equatorial forcing on the extratropics, rather than the other way round. As such, we do not suggest that regressing out the CPCT index pair solves the ENSO removal problem. The above analysis, however, does show that the PMM pattern is sensitive to how ENSO removal is performed.

The PMM definition in model diagnostics

The PMM is often analyzed in climate models, for example in the context of seasonal predictions[16], climate model evaluation[36,37], or climate change[38,39]. Typically, these studies use the reference definition of the PMM, which involves regressing out the CTI from fields and subsequently applying MCA. When performed on observations, the first mode invariably shows the PMM pattern. For model output, on the other hand, this is not necessarily the case, with 15 of the 44 global climate models examined here yielding the PMM as the second or even third MCA mode (Fig. 4a). Climate models tend to feature ENSO variability that extends too far westward[40,41]. This may change the amount of residual ENSO variability after CTI removal and thus shift the PMM-pattern to a higher mode. An important implication is that mechanically applying the reference PMM definition to climate models may yield misleading results because the first MCA mode will be identified as the PMM, whereas in some models the PMM is actually represented by higher modes, as is the case for the widely used CESM2. Therefore, care must be taken to pick the mode that is most similar to the observed PMM (as measured by pattern correlation).

When the PMM is not represented by the first MCA mode, it also tends to be quite different from the corresponding SST PCA (see "Methods"). In other words, in those models, representing the PMM with SST only is less successful than it is for the observations. In the remaining models, however, the correlation between the PMM and the PMM_PCA is invariably above 0.8 and often quite close to 1. Even when the reference PMM and PMM_PCA are poorly correlated, this does not necessarily mean that the MCA adequately represents coupled SST-wind variability; rather, the PCA may partition the residual ENSO variability in a different manner.

When the simple SST area average defined in Fig. 1c (CTI not regressed out) is used to represent PMM variability in the climate models, the correlations with the standard PMM are reasonably high (Fig. 4b), even for those models that have a low correlation between the PMM and PMM_PCA. This indicates that the simple area average provides a relatively robust measure of the PMM.

The reason why some models do not represent the PMM in the first MCA mode deserves further analysis. A PCA analysis of SST in the tropical Pacific provides some clues. For this analysis, no ENSO index is regressed out prior to PCA. Without regressing out ENSO, the PMM-like SST pattern is well represented by the second EOF in the NCEP/NCAR Reanalysis (Fig. 4c) and the majority of the models (Fig. 4d). In the outlier models, however, the second EOF pattern reveals a conspicuous difference in the South Pacific (Fig. 4e): the southeastward branch of warm SST anomalies that is only weakly developed in the observations is quite pronounced in the outlier models and extends toward South America, leading to a V-shaped
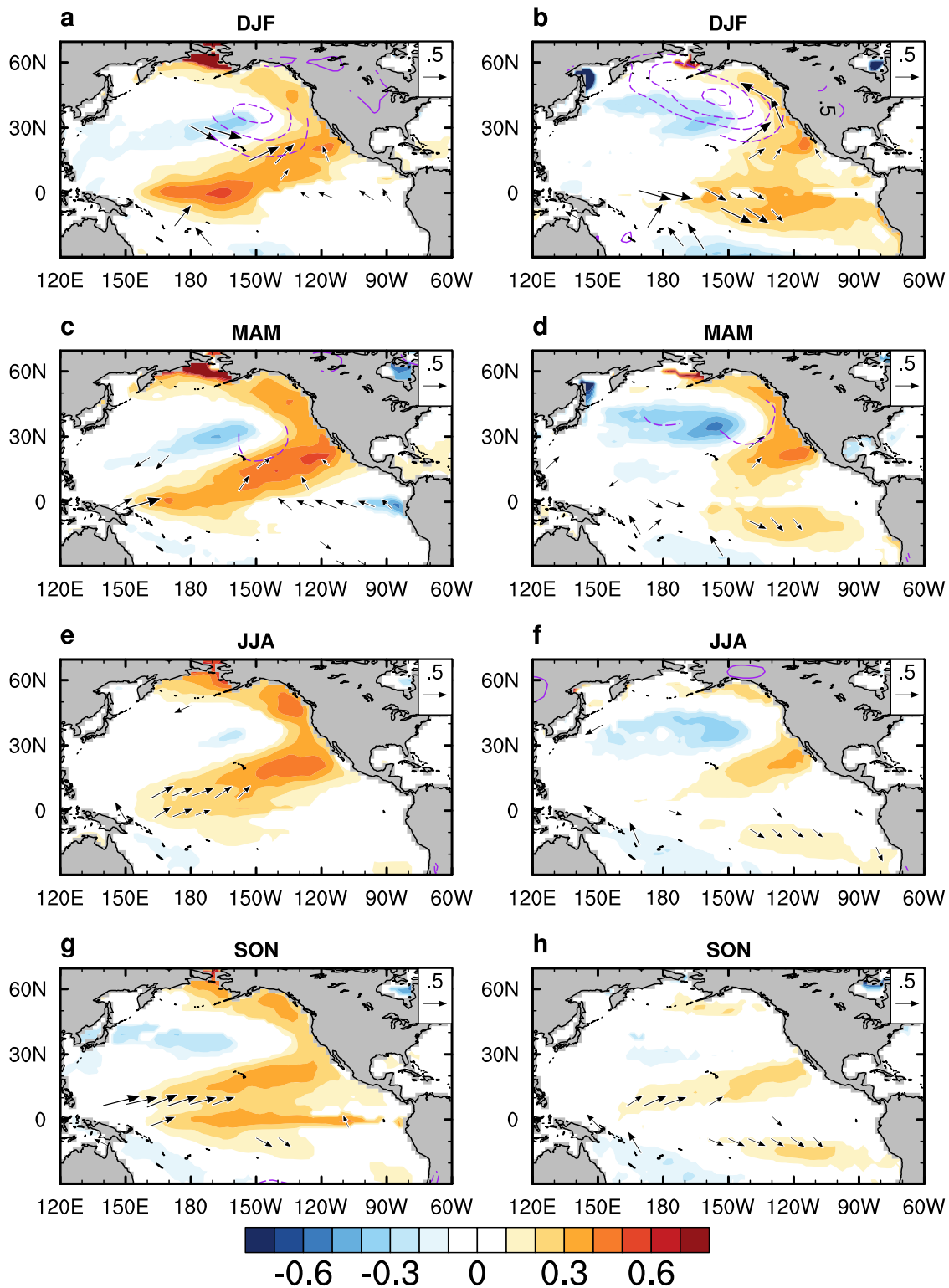
regression of SST, wind, SLP on PMM indices

Fig. 3 Sensitivity to the index used for ENSO removal. a, c, e, g Lagged regressions of anomalous SST (°C, shading), surface winds (m s^{-1}, vectors), and sea-level pressure (contours, interval of 0.25 hPa) onto the MAM reference PMM index. The individual panels show, from top to bottom, seasonal averages for winter (DJF), spring (MAM), summer (JJA), and fall (SON). Only values significant at the 95% confidence level are shown. **b, d, f, h** Like (**a, c, e, g**), but for the PMM_CPCT index, for which the ENSO signal is removed more thoroughly prior to analysis. All fields are from the NCEP/NCAR Reanalysis.
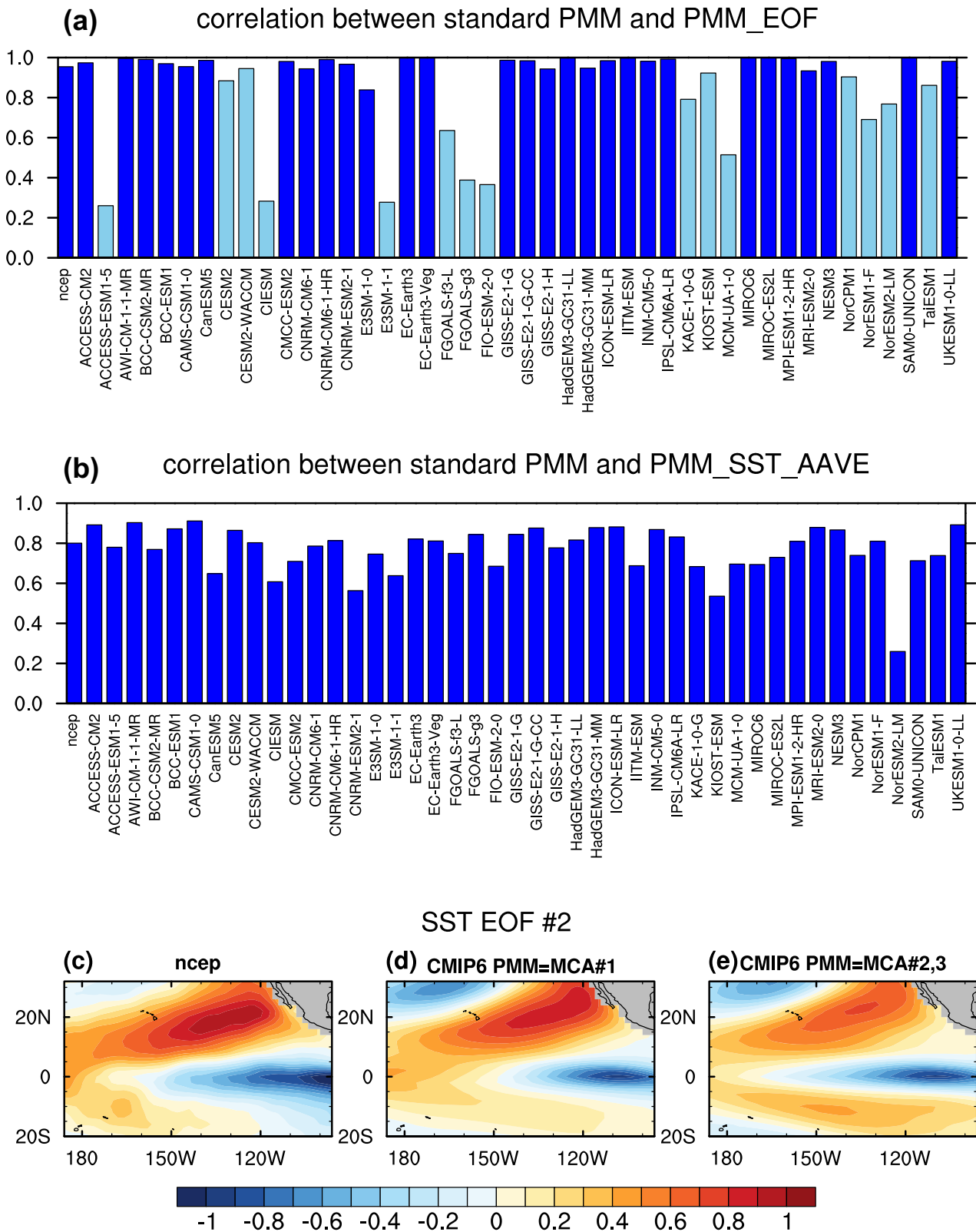
Fig. 4 The PMM index in CMIP6 GCMs. a Correlations between the PMM and the PMM_PCA for the NCEP/NCAR Reanalysis and 44 coupled general circulation model (GCM)s from the CMIP6 intercomparison. For the models, the PMM is taken as the MCA mode that has the highest pattern correlation with the PMM mode of the NCEP/NCAR reanalysis. The models for which this is not the first MCA mode are shaded in light blue. **b** As in (**a**), but for the correlation of the PMM with SST averaged over the area shown in Fig. 1c. **c** Second EOF of the PCA of SST for the NCEP/NCAR reanalysis. **d** As in (**c**) but averaged over the CMIP models for which the PMM is the first MCA mode. **e** As in (**c**) but averaged over the CMIP models for which the PMM is not the first MCA mode (light blue shading in (**a**)). All correlations shown in (**a**) and (**b**) are significant at the 95% confidence level.

pattern that is roughly symmetric about the equator. This results in poor pattern correlations with the reference PMM pattern.

DISCUSSION

Our analysis suggests that the MCA-based reference PMM definition does not reliably identify the wind-SST coupling that is thought to underpin variability in the subtropical North Pacific because it is dominated by SST. Nor does it succeed in effectively removing the influence of ENSO. The resulting PMM index is therefore contaminated by ENSO variability and cannot be interpreted easily as an independent precursor of ENSO. A similar problem surfaces in statistical analyses that derive optimal precursors based on the LIM framework. As these SST precursors resemble the PMM, they already contain part of the ENSO signal[30–32].

The above caveats do not necessarily imply that PMM-like variability cannot serve as a potential precursor to ENSO. Nor does it discount the importance of the WES feedback for the subtropical North Pacific. Those findings are supported by multiple lines of evidence and are most likely robust. For the reasons stated in the above paragraph, however, we believe that the reference PMM definition is not optimally suited to representing the PMM, and that it may overestimate its role as a precursor. Therefore, previous results should be reexamined in two respects: (1) To what extent is the ENSO signal already present during the peak of the PMM (in MAM)? (2) How sensitive is the precursor role of the PMM to the procedure of ENSO removal?

Many studies have suggested a precursor role for the PMM[2–4,7,15–19,42,43] but only a few studies have attempted to quantify this effect in seasonal ENSO predictions[16,22,44]. These studies have found some limited contribution to ENSO prediction skill. While a number of model experiments have been conducted to examine the influence of the PMM on ENSO[22,45,46], more experiments will be needed to quantify the PMM's contribution to ENSO prediction skill, and to assess the role of model biases. These experiments should strive to carefully separate subtropical precursors from ENSO itself.

The conflation of ENSO and subtropical variability in the PMM index can also confound multi-model studies of present and future climate[17,37–39] as intermodel differences in the PMM may just reflect different ENSO characteristics.

To move forward, we suggest using the simple box average of subtropical SST anomalies (indicated in Fig. 1c). The resulting index and regression patterns have some similarity with those of the reference PMM-T index but are not sensitive to how the ENSO influence is removed, or whether it is removed at all (Supplementary Fig. 1c). Moreover, it is relatively robust across most of the climate models examined here. This index can be further refined as shown in Supplementary Fig. 1d. An advantage of using only SST for PMM diagnosis is that SST is more reliably measured and extends further back in time. This allows analyzing longer observational records and, possibly, even paleo proxies. We note that a number of studies have already used alternative definitions of the PMM index that mostly rely on SST[3,4,16].

Ultimately, it would be desirable to have an index that better represents the SST-wind coupling, if this coupling is indeed fundamental to the PMM. Recently, Amaya et al.[47] have shown a promising diagnostic method for a related phenomenon, the Atlantic Meridional mode. Their method does not rely on MCA or PCA but rather uses straightforward correlations of SST and surface wind speed. Application of this method, however, may be more difficult in the Pacific, where the ENSO influence tends to overwhelm other signals. We have performed an analysis along these lines by examining the propagation of SST anomalies from the subtropical North Pacific toward the equator (Supplementary Note 3 and Supplementary Fig. 6). The results, however, only provide very limited support for propagation that is consistent with the WES feedback. This indicates that more analysis will be needed to arrive at a satisfactory diagnostic tool for variability in the subtropical North Pacific.

METHODS

Maximum covariance analysis (MCA) and calculation of the PMM index

Maximum covariance analysis aims to identify pairs of patterns that explain a maximum fraction of covariance among two space-time datasets[21]. The technique is also often referred to as singular value decomposition (SVD) but, to distinguish it from the matrix decomposition method by the same name, we use the term MCA. For all points in the spatial dimensions of the first dataset, MCA calculates the temporal covariance with all points in the second dataset. The resulting covariance matrix is subjected to an eigenvalue decomposition that identifies the spatial patterns explaining the largest fraction of covariance. Temporal expansion coefficients are obtained by projecting the spatial patterns onto the datasets.

The calculation of the reference PMM index follows the method outlined by Chiang and Vimont[1]. For details, please refer to https://www.aos.wisc.edu/~dvimont/MModes/PMM.html. The important steps are summarized here: (1) Take the skin temperature and 10 m wind from the NCEP/NCAR Reanalysis. The analysis region is 175°E to 95°W, 21°S to 32°N, and the analysis period is fixed as 1950–2005. (2) Mask out land points. (3) Calculate the anomalies of all fields, i.e., the deviations from the monthly climatology. (4) Remove the linear trend from all fields. (5) Regress out the cold tongue index (CTI), a measure of ENSO activity, which is defined as SST averaged over 180°-90°W, 6°S-6°N. (6) Calculate the MCA between SST on the one side and the zonal and meridional surface wind components on the other. (7) Repeat steps (1)–(5) but use the entire available period (1948–present). Project the spatial pattern of the first MCA mode onto the SST time series to obtain the temperature PMM index (PMM T). This is the index that is most commonly used in the literature. Projecting the time series of the combined wind components onto first MCA mode of the wind time series yields the wind PMM index (PMM W). Chiang and Vimont[1] suggest that the latter index mixes midlatitude wind forcing with the coupled ocean-atmosphere interaction of the PMM. Thus, the PMM T index is recommended for analyzing coupled PMM variability[48].

We follow exactly the procedure outlined by Chiang and Vimont[1] and perform it on the same dataset (NCEP/NCAR Reanalysis). The resulting reconstructed PMM index agrees very well with the one that is made available by Daniel Vimont on his website[48], with a correlation of 0.99. The slight discrepancy may be due to the details of the software packages used for the MCA calculation. We take this reconstruction of the PMM index as our reference.

Principal component analysis

Principal component analysis (PCA), also known as empirical orthogonal function (EOF) analysis, is similar to MCA but uses only one dataset to calculate the covariances of all spatial data points. The resulting matrix is subjected to an eigenvalue decomposition and the patterns explaining the highest fraction of variability are identified. The spatial patterns are called EOF modes and their expansion coefficients, obtained by projecting the EOFs on the dataset, are called principal components (PCs).

In the present study, we use PCA on the same spatial domain as for the MCA and prepare the dataset in the same manner as for the MCA, using steps (1)–(5) outlined under the description of the MCA.

Linear inverse modeling (LIM)

LIM is an empirical statistical approach that aims to extract the essence of a complex non-linear system from data[30]. If x is the state vector of a subset of the full system, LIM assumes that it can be represented by $dx/dt = Bx + \xi$, where d/dt indicates the time derivative, B is a linear operator, ξ is white noise forcing, and nonlinear terms have been neglected. The linear operator can be estimated by performing essentially a lagged covariance analysis on the data: $B = \tau_0^{-1} ln\{C(\tau_0)C(0)^{-1}\}$, where $C(\tau_0)$ is the covariance matrix at time lag τ_0, and $C(0)^{-1}$ the inverse of the covariance matrix at lag 0. Based on the linear operator B, optimal precursors can be calculated through an eigenvalue analysis. The state vector x can represent a single variable, such as SST, or a collection of different variables. In order to facilitate the matrix calculations, LIM is usually performed on a set of leading principal components from a PCA.

Statistical significance tests

A two-sided Student's t-test is used to determine the statistical significance of correlation and regression coefficients. Serial correlation is accounted for by calculating the effective sample size.

The statistical significance of MCA modes is calculated using a bootstrapping approach[49]. One-year blocks of the wind data are randomly permuted to generate 1000 scrambled time series, so that the temporal relation between wind and SST is lost. It is then determined how many of the scrambled MCAs yield a statistic larger than that of the original, unscrambled time series. This number is divided by the number of permutations to obtain the P-value. The statistics that are typically examined for a given mode include the explained squared covariance fraction, the correlation between the expansion coefficients, and the singular value. Of these, the singular value is typically recommended and is the measure used in the present study.

Observation-based data

We use the National Centers for Environmental Prediction/National Center for Atmospheric Research (NCEP/NCAR) Reanalysis product[50] as our observation-based dataset. Reanalyses are climate model simulations that are constrained by observations from many different sources (in-situ, satellite, radiosondes etc.) to obtain a best estimate of the true state of the atmosphere that is gap-free in time and space. The NCEP/NCAR Reanalysis is chosen as it is the dataset used to define the reference PMM index. Using other datasets yields very similar results. The analysis period is 1950–2005, the same as the one used for the definition of the reference PMM on the PMM website[48].

Model output

We use output from the preindustrial control experiment (piControl) of the Coupled Model Intercomparison Project Phase 6 (CMIP6)[51]. piControl is chosen as it offers long time series under steady radiative forcing. The 44 models chosen for our analysis are listed in the Supplementary Table 1.

ENSO indices

Many measures of ENSO activity have been devised. These are usually simple area averages of equatorial Pacific SST. Chiang and Vimont[1] use the cold tongue index (CTI), defined as SST averaged over the region 180°-90°W and 6°S-6°N, to regress out the ENSO influence prior to their MCA. This measure is indeed a good indicator of the canonical ENSO, that is most pronounced in the eastern equatorial Pacific and also called cold tongue (CT) ENSO. It does, however, not take into account SST off the Peruvian coast. More importantly, it does not include ENSO variability west of the date line, which is referred to as El Niño Modoki[28] or Western Pacific (WP) ENSO[29]. Takahashi et al.[29] suggest using a pair of indices to account for both the CT and WP flavors of ENSO. One of their suggestions relies on the well-established Niño 4 (SSTs averaged over 160°E-150°W, 5°S-5°N) and Niño 1+2 (SSTs averaged over 90°-80°W, 10°S-0) indices. These two indices are linearly combined to yield a pair of roughly orthogonal indices: C = 1.7*Nino4 – 0.1*Nino12, and E = Nino12 – 0.5*Nino4. We use this index pair to perform a more complete ENSO removal prior to the calculation of the PMM index. We refer to the PMM index modified in this way as the PMM_CPCT.

The Wind-Evaporation-SST (WES) feedback

A coupled air-sea feedback loop, in which a weakening of the subtropical trade winds causes a reduction of sea-surface evaporation[11,12]. This reduces the cooling by latent heat flux and results in a warming of the underlying SSTs. The resulting warm SST anomalies influence the large-scale atmospheric circulation so as to further reduce the strength of the trade winds. Since the weakening of the trades is most pronounced equatorward of the SST anomalies, it has been suggested that the pattern slowly propagates equatorward. The WES feedback relies on thermodynamic processes. This sets it apart from the Bjerknes feedback in the equatorial Pacific, which depends on subsurface ocean dynamics.

REFERENCES

1. Chiang, J. C. & Vimont, D. J. Analogous Pacific and Atlantic meridional modes of tropical atmosphere–ocean variability. J. Clim. 17, 4143–4158 (2004).
2. Chang, P. et al. Pacific meridional mode and El Niño-Southern oscillation. Geophys. Res. Lett. 34 https://doi.org/10.1029/2007GL030302 (2007).
3. Zhang, H., Deser, C., Clement, A. & Tomas, R. Equatorial signatures of the Pacific meridional modes: dependence on mean climate state. Geophys. Res. Lett. 41, 568–574 (2014).
4. Di Lorenzo et al. ENSO and meridional modes: a null hypothesis for Pacific climate variability. Geophys. Res. Lett. 42, 9440–9448 (2015).
5. Di Lorenzo, E. & Mantua, N. Multi-year persistence of the 2014/15 North Pacific marine heatwave. Nat. Clim. Change 6, 1042–1047 (2016).
6. Zhang, W., Vecchi, G. A., Murakami, H., Villarini, G. & Jia, L. The Pacific meridional mode and the occurrence of tropical cyclones in the western North Pacific. J. Clim. 29, 381–398 (2016).
7. Zhao, J., Kug, J.-S., Park, J.-H. & An, S.-I. Diversity of North Pacific Meridional Mode and its distinct impacts on El Niño-Southern Oscillation. Geophys. Res. Lett. 47, e2020GL088993 (2020).
8. Neelin, J. D. et al. ENSO theory. J. Geophys. Res. 103, 14261–14290 (1998).
9. Chang, P. et al. Climate fluctuations of tropical coupled systems—the role of ocean dynamics. J. Clim. 19, 5122–5174 (2006).
10. McPhaden, M. J., Santoso, A. & Cai, W. (editors) El Niño Southern Oscillation in a Changing Climate. https://doi.org/10.1002/9781119548164 (2020).
11. Xie, S.-P. & Philander, S. G. H. A coupled ocean-atmosphere model of relevance to the ITCZ in the eastern Pacific. Tellus 46A, 340–350 (1994).
12. Chang, P., Ji, L. & Li, H. A decadal climate variation in the tropical Atlantic Ocean from thermodynamic air-sea interactions. Nature 385, 516–518 (1997).
13. Wang, S. Y., Hipps, L., Gillies, R. R. & Yoon, J. H. Probable causes of the abnormal ridge accompanying the 2013–2014 California drought: ENSO precursor and anthropogenic warming footprint. Geophys. Res. Lett. 41, 3220–3226 (2014).

14. Murakami, H. et al. Dominant role of subtropical Pacific warming in extreme eastern Pacific hurricane seasons: 2015 and the future. *J. Clim.* **30**, 243–264 (2017).

15. Larson, S. & Kirtman, B. The Pacific meridional mode as a trigger for ENSO in a high-resolution coupled model. *Geophys. Res. Lett.* **40**, 3189–3194 (2013).

16. Larson, S. M. & Kirtman, B. P. The Pacific meridional mode as an ENSO precursor and predictor in the North American multimodel ensemble. *J. Clim.* **27**, 7018–7032 (2014).

17. Lin, C. Y., Yu, J. Y. & Hsu, H. H. CMIP5 model simulations of the Pacific meridional mode and its connection to the two types of ENSO. *Int. J. Clim.* **35**, 2352–2358 (2015).

18. Ogata, T., Doi, T., Morioka, Y. & Behera, S. K. Mid-latitude source of the ENSO-spread in SINTEX-F ensemble predictions. *Clim. Dyn.* **52**, 2613–2630 (2019).

19. Alexander, M. A., Vimont, D. J., Chang, P. & Scott, J. D. The impact of extratropical atmospheric variability on ENSO: Testing the seasonal footprinting mechanism using coupled model experiments. *J. Clim.* **23**, 2885–2901 (2010).

20. McPhaden, M. J. Tropical Pacific Ocean heat content variations and ENSO persistence barriers. *Geophys. Res. Lett.* **30**, 1480 (2003).

21. Bretherton, C. S., Smith, C. & Wallace, J. M. An intercomparison of methods for finding coupled patterns in climate data. *J. Clim.* **5**, 541–560 (1992).

22. Amaya, D. J. The Pacific Meridional Mode and ENSO: a review. *Curr. Clim. Change Rep.* **5**, 296–307 (2019).

23. Stuecker, M. F. Revisiting the Pacific meridional mode. *Sci. Rep.* **8**, 1–9 (2018).

24. Bjerknes, J. Atmospheric teleconnections from the equatorial Pacific. *Mon. Weather. Rev.* **97**, 163–172 (1969).

25. Newman, M. & Sardeshmukh, P. D. A caveat concerning singular value decomposition. *J. Clim.* **8**, 352–360 (1995).

26. Cherry, S. Singular value decomposition analysis and canonical correlation analysis. *J. Clim.* **9**, 2003–2009 (1996).

27. Wallace, J. M., Mitchell, T. P. & Deser, C. The influence of sea surface temperature on surface wind in the eastern equatorial Pacific: seasonal and interannual variability. *J. Clim.* **2**, 1492–1499 (1989).

28. Ashok, K., Behera, S. K., Rao, S. A., Weng, H. & Yamagata, T. El Niño Modoki and its possible teleconnection. *J. Geophys. Res.* **112**, C11007 (2007).

29. Takahashi, K., Montecinos, A., Goubanova, K. & Dewitte, B. ENSO regimes: reinterpreting the canonical and Modoki El Niño. *Geophys. Res. Lett.* **38** https://doi.org/10.1029/2011GL047364 (2011).

30. Penland, C. & Sardeshmukh, P. D. The optimal growth of tropical sea surface temperature anomalies. *J. Clim.* **8**, 1999–2024 (1995).

31. Alexander, M. A., Matrosova, L., Penland, C., Scott, J. D. & Chang, P. Forecasting Pacific SSTs: linear inverse model predictions of the PDO. *J. Clim.* **21**, 385–402 (2008).

32. Vimont, D. J., Alexander, M. A. & Newman, M. Optimal growth of Central and East Pacific ENSO events. *Geophys. Res. Lett.* **41**, 4027–4034 (2014).

33. Martinez-Villalobos, C. & Vimont, D. J. An analytical framework for understanding tropical meridional modes. *J. Clim.* **30**, 3303–3323 (2017).

34. Carranza, L. Contra-corriente maritime, observada en Paita y Pacasmayo. *Bol. Soc. Geogr. Lima* **1**, 344–345 (1892).

35. Carrillo, C. N. Hidrografía Oceánica: Disertación sobre las corrientes oceánicas y estudios de la corriente peruana ó de Humboldt. *Bol. Soc. Geogr. Lima* **2**, 72–110 (1893).

36. Park, J. H. et al. Role of the climatological intertropical convergence zone in the seasonal footprinting mechanism of El Niño–Southern Oscillation. *J. Clim.* **34**, 5243–5256 (2021).

37. Zheng, Y., Chen, W. & Chen, S. Intermodel spread in the impact of the springtime Pacific Meridional Mode on following-winter ENSO tied to simulation of the ITCZ in CMIP5/CMIP6. *Geophys. Res. Lett.* **48**, e2021GL093945 (2021).

38. Liguori, G. & Di Lorenzo, E. Meridional modes and increasing Pacific decadal variability under anthropogenic forcing. *Geophys. Res. Lett.* **45**, 983–991 (2018).

39. Jia, F., Cai, W., Gan, B., Wu, L. & Di Lorenzo, E. Enhanced North Pacific impact on El Niño/Southern Oscillation under greenhouse warming. *Nat. Clim. Change* **11**, 840–847 (2021).

40. Li, G. & Xie, S.-P. Tropical biases in CMIP5 multimodel ensemble: The excessive equatorial Pacific cold tongue and double ITCZ problems. *J. Clim.* **27**, 1765–1780 (2014).

41. L'Heureux, M. L. et al. ENSO prediction. In McPhaden, M. J., Santoso, A. Cai, W. (Eds.), *El Niño Southern Oscillation in a Changing Climate*, Washington, DC: American Geophysical Union 227–246 (2020).

42. Anderson, B. T., Perez, R. C. & Karspeck, A. Triggering of El Niño onset through trade wind-induced charging of the equatorial Pacific. *Geophys. Res. Lett.* **40**, 1212–1216 (2013).

43. Ma, J., Xie, S. P. & Xu, H. Contributions of the North Pacific meridional mode to ensemble spread of ENSO prediction. *J. Clim.* **30**, 9167–9181 (2017).

44. Fan, H., Huang, B., Yang, S. & Dong, W. Influence of the Pacific Meridional Mode on ENSO evolution and predictability: asymmetric modulation and ocean preconditioning. *J. Clim.* **34**, 1881–1901 (2021).

45. Lu, F. & Liu, Z. Assessing extratropical influence on observed El Niño–Southern Oscillation events using regional coupled data assimilation. *J. Clim.* **31**, 8961–8969 (2018).

46. Liguori, G. & Di Lorenzo, E. Separating the North and South Pacific Meridional Modes contributions to ENSO and tropical decadal variability. *Geophys. Res. Lett.* **46**, 906–915 (2019).

47. Amaya, D. J., DeFlorio, M. J., Miller, A. J. & Xie, S.-P. WES feedback and the Atlantic meridional mode: observations and CMIP5 comparisons. *Clim. Dyn.* **49**, 1665–1679 (2017).

48. Daniel Vimont's PMM website: https://www.aos.wisc.edu/~dvimont/MModes/PMM.html

49. Czaja, A. & Frankignoul, C. Observed impact of Atlantic SST anomalies on the North Atlantic Oscillation. *J. Clim.* **15**, 606–623 (2002).

50. Kalnay, E. et al. The NCEP/NCAR 40-year reanalysis project. *Bull. Am. Meteorol. Soc.* **77**, 437–472 (1996).

51. Eyring, V. et al. Overview of the Coupled Model Intercomparison Project Phase 6 (CMIP6) experimental design and organization. *Geosci. Model Dev.* **9**, 1937–1958 (2016).

AUTHOR CONTRIBUTIONS

I.R. and M.F.S. conceived the central idea of the study. I.R. conducted the analysis and wrote the initial draft. All authors were involved in interpreting the results and contributed to improving the manuscript.

COMPETING INTERESTS

The authors declare no competing interests.

ADDITIONAL INFORMATION

Supplementary information The online version contains supplementary material available at https://doi.org/10.1038/s41612-022-00317-8.

Correspondence and requests for materials should be addressed to Ingo Richter.

Reprints and permission information is available at http://www.nature.com/reprints

Publisher's note Springer Nature remains neutral with regard to jurisdictional claims in published maps and institutional affiliations.